PCCP

PAPER

View Article Online
View Journal | View Issue

Cite this: *Phys. Chem. Chem. Phys.*, 2017, **19**, 5222

A new approach to distance measurements between two spin labels in the >10 nm range

A. Blank

ESR spectroscopy can be efficiently used to acquire the distance between two spin labels placed on a macromolecule by measuring their mutual dipolar interaction frequency, as long as the distance is not greater than ~10 nm. Any hope to significantly increase this figure is hampered by the fact that all available spin labels have a phase memory time (T_m), restricted to the microseconds range, which provides a limited window during which the dipolar interaction frequency can be measured. Thus, due to the inverse cubic dependence of the dipolar frequency over the labels' separation distance, evaluating much larger distances, *e.g.* 20 nm, would require to have a T_m that is ~200 microsecond, clearly beyond any hope. Here we propose a new approach to greatly enhancing the maximum measured distance available by relying on another type of dipole interaction-mediated mechanism called spin diffusion. This mechanism operates and can be evaluated during the spin lattice relaxation time, T_1 (commonly in the milliseconds range), rather than only during T_m. Up until recently, the observation of spin diffusion in solid electron spin systems was considered experimentally impractical. However, recent developments have enabled its direct measurement by means of high sensitivity pulsed ESR that employs intense short magnetic field gradients, thus opening the door to the subsequent utilization of these capabilities. The manuscript presents the subject of spin diffusion, the ways it can be directly measured, and a theoretical discussion on how intramolecular spin-pair distance, even in the range of 20–30 nm, could be accurately extracted from spin diffusion measurements.

Received 7th November 2016,
Accepted 27th January 2017

DOI: 10.1039/c6cp07597e

rsc.li/pccp

1. Introduction

Distance determination between two electron spin labels is arguably one of the most significant applications of modern electron spin resonance spectroscopy. Methods such as double electron–electron resonance technique (DEER),[1] double quantum coherence (DQC),[2] or single-frequency technique for refocusing (SIFTER),[3] aim at measuring the distance distribution and possibly extracting the mean distance between two spin labels positioned on a large molecule or supramolecular structure. This technique has led in recent years to numerous publications, mostly related to issues of advanced structural biology issues.[4–10] Furthermore, all these dipolar ESR spectroscopy approaches are constantly being improved, mainly through more optimized pulse sequences,[11] better spin labels,[12,13] low-γ isotopically enriched molecules and solvents,[14] and optimized high-end spectrometers,[15] with the goal of increasing the maximum measurable distance between the two labels. However, despite these extensive efforts, DEER and related techniques are limited to the measurement of distances up to ~10 nm, with not much hope of significantly increasing this barrier. The reason for this limitation can be understood by examining a typical DEER sequence (Fig. 1a). In DEER experiments (and the same is applicable to DQC and other related techniques),

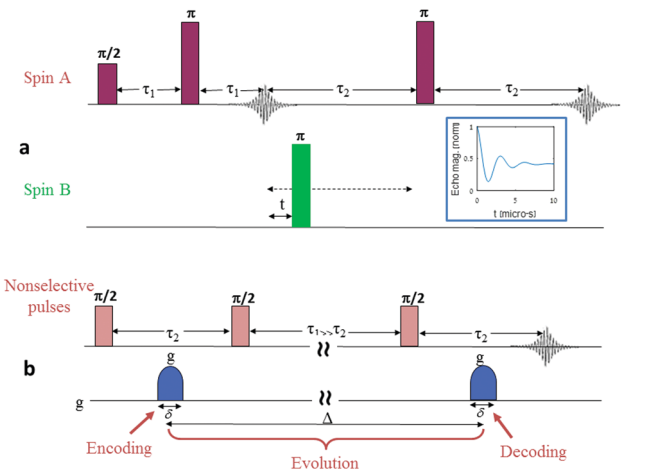

Fig. 1 (a) Typical four-pulse DEER sequence. The observable spin A evolves during the sequence only in the transverse (XY) laboratory plane and thus its signal can be recorded as long as the timed duration of the sequence is not much larger than T_m. The inset shows a typical DEER dipolar signal of the echo magnitude as a function of t. (b) Pulsed gradient spin echo (PGSE) sequence for measuring spin diffusion.

Schulich Faculty of Chemistry, Technion – Israel Institute of Technology, Haifa, 3200003, Israel. E-mail: ab359@technion.ac.il

the information regarding the intramolecular spin labels' separation distance is obtained by measuring the frequency of the dipolar interaction between the two spins. This frequency, ν_{dipolar}, is directly linked to the intramolecular spin-pair distance, d, *via* the expression:

$$\nu_{\text{dipolar}} \approx \frac{52.2\ [\text{MHz}]}{d^3\ [\text{nm}^3]} \tag{1}$$

Here, we assume that both dipolar coupled electrons have a g factor of ~ 2 and neglect the relative angular orientation between the spins, to represent the order of magnitude of this frequency. Thus, in order to extract the distance, a good knowledge of ν_{dipolar} is required. The period of the dipolar interaction frequency is limited by the phase memory time (T_{m}) of the measured spin labels. Usually, observations of at least 2–3 oscillations of the dipolar interaction frequency in the DEER time-domain plot (Fig. 1a) would be necessary in order to provide the intramolecular spin distance with reasonable accuracy.[16] More exact and rigorous analysis (using such tools as DEER analysis[17] or the Tikhonov regularization method[18]) may be implemented on the DEER data in order to extract more accurately both the mean distance and its distribution. However, these methods also cannot escape the problem of a short-time observation window that limits the maximum measurable intramolecular spin distance. Furthermore, due to the $1/d^3$ dependence of the dipolar interaction frequency, doubling the available measured distance, let's say from 10 nm to 20 nm, would require a T_{m} that is 8 times longer. Thus, this approach has clearly hit a brick wall with respect to the prospects of significantly increasing the measured intramolecular spin distance.

Here we present and theoretically analyse an alternative approach that has the potential to significantly increase the upper measurable distance limitation to the range of a few tens of nanometers. This approach, as in the case of DEER, is also based on measuring processes that are mediated by the dipolar interaction between the two spin labels. However, the main difference is that it examines processes that occur within T_1 and not in the T_{m} time scale, which for most systems of relevance (*e.g.*, nitroxides, Gd ions, trityls) can be more than 3–4 orders of magnitude longer at the cryogenic temperatures commonly employed in DEER and DQC.[19] The physical phenomena that can be monitored and relied upon is spin diffusion. The next section will provide more details about spin diffusion and how it can be measured (relying on our recent work, where for the first time we experimentally measured the spin diffusion of electron spins in a solid sample[20]). Following this, it will be shown how the information on spin diffusion can directly lead to finding the distance between two spin labels. Several quantitative simulated data are provided to support these claims, as well as a description of the experimental capabilities required to enable spin diffusion and intramolecular spin distance measurements in the range of a few tens of nanometers.

2. Spin diffusion and its measurements

The concept of spin self-diffusion and the spin diffusion coefficient, D_{s}, was introduced a long time ago by Bloembergen in a seminal paper.[21] Spin diffusion is a pure quantum mechanical process where the wavefunction of the spins diffuses across the sample from spin to spin, just as in conventional diffusion, but without any actual spatial motion by the spins. It is based on the fact that two interacting spins with $|\uparrow\rangle$ and $|\downarrow\rangle$ states can interchange their states to $|\downarrow\rangle$ and $|\uparrow\rangle$ states, a process commonly referred to as a "flip-flop". The spin–spin interaction leading to such flip-flop event can occur either *via* a dipolar or an exchange mechanism, or both, with the former being more relevant to our case of electron spin diffusion. For identical spins, this flip-flop is energy-preserving and occurs stochastically with an average exchange rate, W, that strongly depends on the spin–spin interaction strength. Even if the energies of the two spins are not identical, the flip-flop can still occur very effectively, provided that the dipolar interaction is at least in the order of the energy difference between the spins.[22] Calculations or measurements of W are far from trivial, especially in dilute electron spin systems. In principle, W_{jk}, (the exchange rate between spins j and k) can be calculated from first principles, assuming that the dipole interaction is a small perturbation to the Hamiltonian:[21–24]

$$W_{jk} = \frac{\pi}{2}\left[\frac{\mu_0}{4\pi}\frac{\hbar\gamma_j\gamma_k}{{d_{jk}}^3}\right]^2\left[\frac{3\cos^2\theta_{jk}-1}{2}\right]^2 f_{jk}(0) \tag{2}$$

where d_{jk} is the distance between spins j and k, and θ_{jk} is the angle between d_{jk} and the direction of B_0. However, such calculations are limited by nature since they require *a priori* data about the zero-quantum transition normalized spectral line shape function on the two-spin system, $f_{jk}(\omega)$, with possible influences by other neighboring species. An alternative way to present eqn (2) is to include all constants, as well as the sample and temperature-dependent value of $f_{jk}(0)$ in a single constant and retain only the distance and orientation dependence of W_{jk}:

$$W_{jk} = {K_{\text{ex}}}^2(3\cos^2\theta_{jk} - 1)^2/{d_{jk}}^6 \tag{3}$$

where K_{ex} is a constant that depends on the type of sample and the temperature used.

For the sake of completeness of presentation, we briefly provide here the approximate analytical expression relating W to the spin diffusion coefficient, D_{s}, (using the approach of Bloembergen[21] and those who followed his work). We assume a sample with $S = 1/2$ spins that are located on a cubic lattice with equal spacing a, and have an equal nearest neighbor flip-flop rate $W = W_{jk}$ between spins j and k (assuming no other flip-flop events). We denote the polarization $p(x,t) = P_+(x,t) - P_-(x,t)$, where $P_{+(-)}(x,t)$ is the probability of finding at x and at time t, a $|+1/2\rangle$ ($|-1/2\rangle$) state. Thus, based on the definition of W, it is possible to write that:

$$\begin{aligned}\frac{-\partial p(x,t)}{\partial t} = W\{&P_+(x+a,t)P_-(x,t) - P_+(x,t)P_-(x-a,t)\\ &+ P_+(x-a,t)P_-(x,t) - P_+(x,t)P_-(x+a,t)\}\end{aligned} \tag{4}$$

Using the relation $P_+(x,t) + P_-(x,t) = 1$ and neglecting terms that are quadratic in p results in the well-known diffusion equation:

$$\frac{-\partial p(x,t)}{\partial t} = D_{\text{s}}\frac{\partial^2 p}{\partial x^2};\quad D_{\text{s}} = Wa^2 \tag{5}$$

Therefore, the flip-flop events lead to a phenomenon that is identical to conventional real-space diffusion. Accordingly, the measurement of spin diffusion can be carried out using methods that are identical to those employed in the past (and still extensively used today) to measure real-space diffusion. In NMR such methods have been standard practice for many years. Real space diffusion of proton spins can be accurately measured employing NMR echo sequences in the presence of a static or pulse magnetic field gradient. For example, a very common pulse sequence for performing such measurements is the pulsed gradient spin echo sequence (PGSE), shown in Fig. 1b. The magnitude of the echo signal acquired *via* this sequence is given by the Stekel–Tanner equation:[25]

$$E^{g}_{(t=2\tau_2+\tau_1)} = A\exp\left(-2\tau_2/T_m - \tau_1/T_1 - D_s\gamma^2 g^2\delta^2(\Delta-\delta/3)\right) \quad (6)$$

In a sample with diffusing species, *e.g.*, molecules in liquids, this leads to a significant reduction in the echo signal's magnitude, which can be directly linked to the diffusion coefficient of the spins.[26–29] Measuring the diffusion of the spins' wave function due to the flip-flop mechanism when the spins are physically fixed in a solid is far less common. However, there are some unique examples of just such measurements, but only in the field of NMR, where spins are closely spaced and relaxation times are relatively very long.[30–33] In the case of electron spins, the measurement of self-diffusion, both in real space and certainly for physically fixed spins, is far less common. The reason for this lies in the technical difficulties that arise due to the short relaxation times of the electron spins, which in turn pose extreme challenges to the required magnitude and duration of the applied magnetic field gradients. Physical real-space diffusion was measured in the past in the unique case of conduction electrons in solids, thanks to their relatively large diffusion coefficient of $D_s > 10^{-6}$ m^2 s^{-1}.[34] More recently, a much more advanced setup using a unique set including a miniature resonator and gradient coils, driven by powerful and fast gradient drivers, was employed to measure physical electron spin diffusion in liquids, with D_s as low as 10^{-10} m^2 s^{-1}.[35–37] The diffusion of the electron spins' wave function in solids (due exclusively to flip-flops) was measured only very recently by our group. Experiments with a sample of phosphorus-doped single crystal of ^{28}Si were successful, showing typical D_s values of only $\sim 10^{-14}$ m^2 s^{-1}, while for a sample of NV centers in diamond the results were not conclusive.[20]

3. Finding the distance between two spin labels *via* spin diffusion measurements

With a PGSE sequence, the measured echo decay due to diffusion can be explored as a function of two different parameters: the evolution time, Δ, and the strength of the pulsed field gradients, g (as reflected by eqn (6)). Interestingly, according to eqn (6), there is no real difference between these two parameters and both would lead to the same phenomenon of echo decay. However, this is misleading, since eqn (6) was originally developed to describe the effect of classical diffusion in real space with a homogenous sample assuming a continuous medium filled with spins. In our case of solid samples with physically fixed electron spins, the behavior of the echo decay due to changes in Δ and g would be quite different and thus the well-known Stekel–Tanner equation must be revisited.

In order to qualitatively understand the reasons for deviations from the Stekel–Tanner prediction when treating samples of relevance to our present theme, let us assume the case of a solid solution of doubly-labeled macromolecules, that have a fixed intramolecular spin-pair distance of 20 nm and a mean intermolecular distance of 135 nm (corresponding 4×10^{14} molecules per cm^3, or to a concentration of $\sim$0.66 μM). We now assume that we apply the pulse sequence of Fig. 1b and observe the echo decay due to spin diffusion as a function of the evolution time, Δ, for two types of gradient pulses, both of them with a duration of δ = 2 μs, but the first one with g = 290 T m^{-1} and the second one with g = 1460 T m^{-1}. These gradient pulses correspond to values of $\lambda = 2\pi/q \approx$ 100 and 20 nm, respectively (where q is defined as $q = \gamma\delta g$[29]). Based on the predictions of eqn (6), it seems that as we step up Δ, we should observe a meaningful exponential decay of the echo signal. In practice, due to the discreteness of the spins' locations, and the fact that there are two very different scales of distances in the sample (the intramolecular spin-pair distance of 20 nm and the intermolecular distance of 135 nm) the behavior of the decay curve will be non-exponential, as can be seen in Fig. 2. The results of Fig. 2 are based on a numerical simulation whose details are provided in the Appendix. The "noise" is due to the relatively small number of molecules used in the simulation (100 spin pairs, but with

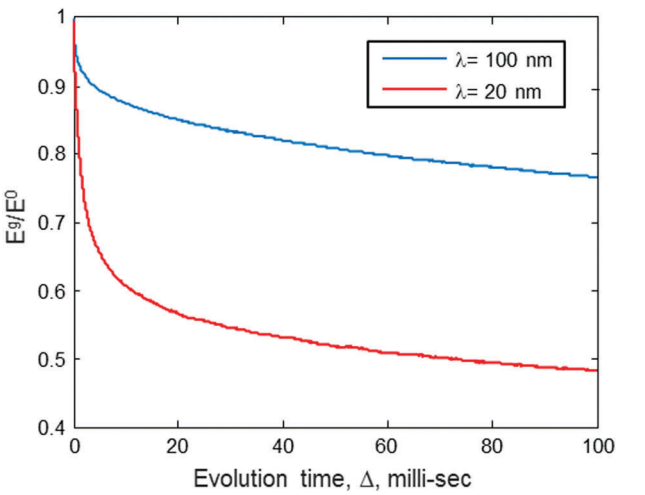

Fig. 2 The ratio of the stimulated echo acquired by the sequence in Fig. 1b with gradient E^g, to that without gradient E^0, as a function of the evolution time, Δ, for two values of gradients (corresponding to two different λ values). Results are based on numerical simulation (Appendix). The simulation assumes a sample with a molecular concentration of 4×10^{14} molecules per cm^3 (0.66 μM), an intramolecular spin-pair distance of d = 20 nm, and $K_{ex} = 3.35 \times 10^5$ Hz nm^3.

each calculation repeated 1000 times) to keep the calculation time reasonable (about 1 h for each evolution graph in Fig. 2 on an Intel i7 2.7 GHz machine).

The behavior seen in Fig. 2 can be explained in the following manner: the λ value of the gradient pulses implies that spins must diffuse to a distance of $\sim\lambda/2$ so that their phases, due to the gradient pulse, would be different enough to affect the echo signal's magnitude. The first $\lambda = 100$ value that we chose is well above 20 nm, meaning that diffusion can be observed only if it is over distances of $\sim$50 nm or more. Namely, a diffusion to a distance of only 20 nm (as is the spin-pair distance of the doubly spin-labeled molecule) would not generate any appreciable echo decay. Thus, a drop of only $\sim$5% in the echo signal is observed as a rapid exponential decay during relatively short values of Δ. Furthermore, in solid-state samples (*e.g.*, frozen solutions), spin diffusion occurs only through discrete "jumps" between spin to spin. The rate of these jumps, W, is proportional to $1/r^6$ (see eqn (2)), and at a spin–spin distance of $r = 135$ nm it is expected to be much less than 1 Hz. (Please note that our recent results show that $W(r = 46\text{ nm}) \sim 10$ Hz.[20]) Thus, during a relatively short evolution time ($\Delta \ll 1/W(r = 135\text{ nm})$), it is highly unlikely that spins would "jump" all the way to the "extra-molecular" space between molecules. Clearly, under the conditions and gradient values we specified above, it would not be possible to observe any appreciable echo decay in our sample, even for Δ of $\sim$10 ms. In longer evolution times, the slow exponential decay would be seen because of intermolecular spin diffusion (the molecules are randomly distributed with a mean distance of 135 nm).

Contrary to what occurs at $\lambda \sim 100$ nm, if we increase the value of g, making $\lambda \sim 20$ nm, then even for Δ of $\sim$10 ms we should be seeing an appreciable echo decay – evidence of the spin diffusion phenomenon (Fig. 2, red curve). In longer evolution times, we experience a similar slow exponential decay as observed at the lower gradient value, since both values of $\lambda \sim 100$ and $\lambda \sim 20$ are smaller than the mean intermolecular distance. This anomalous diffusion behavior (bi-exponential decay) is exactly the phenomena we can make use of to find the intramolecular distance between the spin pairs. Namely, if we choose to use a moderate evolution time $1/W(r = 20\text{ nm}) \ll \Delta \ll 1/W(r = 135\text{ nm})$, and then start a series of experiments while increasing the gradients g (or δ), at some point λ will start to be in the order of the intramolecular spin-pair distance and we would see a dramatic decrease in the echo magnitude. Based on this observation, we could extract the intramolecular spin-pair distance, d.

This λ-dependent anomalous onset behavior is depicted in Fig. 3, which shows the results of the numerical simulation for another sample concentration, also in the case of a doubly spin-labeled molecule with a fixed intramolecular spin-pair distance $d = 20$ nm. The results show a clear decay of the echo signal due to spin diffusion. It is evident that at $\lambda \gg d$ the gradients have a relatively small effect on the echo signal. When approaching the range of $\lambda \sim 2d$ the signal drops in a much more pronounced manner. However, a further increase in the gradients (corresponding to smaller λ values) does not change much the decay curve, with

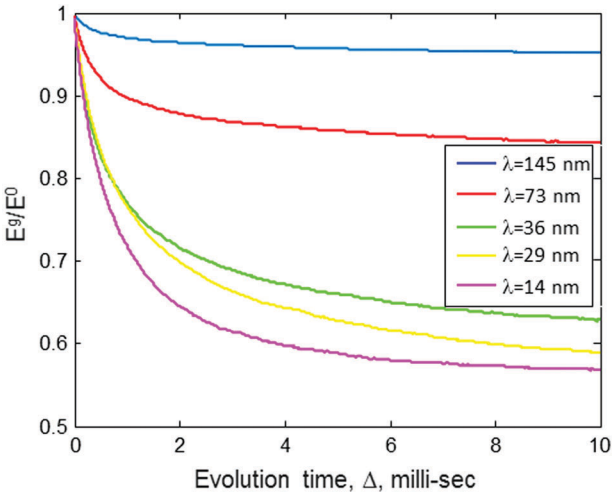

Fig. 3 Numerical simulation of E^g/E^0 as a function of evolution time for various gradient values g, corresponding to various values of λ ($\lambda = 2\pi/\gamma\delta g$). The simulation assumes a sample with a molecular concentration of 10^{14} molecules per cm^3 (0.16 μM), an intramolecular spin-pair distance of $d = 20$ nm, and $K_{ex} = 3.35 \times 10^5$ Hz nm^3.

the initial decay limited to E^g/E^0 of $\sim$0.5. This kind of behavior basically conforms to the description provided above, where a relatively short 10 ms evolution period is not enough to allow spin diffusion to cross the relatively large intermolecular distance of $\sim$200 nm in this example. This prevents any appreciable echo decay during this time frame from intermolecular sources at both small and also large λ values. However, at small λ values there is a significant rapid decay from intramolecular sources with an initial decay down to E^g/E^0 of $\sim$0.5, but not to a lower value, because spin diffusion within the closely-spaced pair is almost completely reversible (flip-flops to both directions), as they are almost completely isolated with polarization leaking out slowly to the intermolecular space. A further reduction in λ cannot change the echo signal significantly since the maximum effects of spin diffusion (distribution of initial spin polarization equally between the two closely-spaced spins) have already been reached with $\lambda \sim d$, and there are no spins that are closer than d and would be further affected by λ reduction.

This type of behavior can be exploited in order to deduce the intramolecular spin-pair distance, d, from the experimental data. One possible way to approach this it is to acquire the E^g/E^0 data for various values of g (which is inversely proportional to λ), but just for a specific, yet still plausible evolution period (*e.g.*, 10 ms in our present example), and then plot the level of the signal at this evolution time point as a function of λ. This form of data analysis leads to the curves shown in Fig. 4. It is clear that as the intramolecular spin-pair distance on a molecule, d, is reduced, larger gradients (smaller λ values) are required to reach a regime of an appreciable decay.

The nature and the form of the type of E^g/E^0 *vs.* λ plots shown in Fig. 4 depend only on three parameters: the intra-molecular spin-pair distance, d, the sample concentration, C, and the flip-flop rate constant, K_{ex}. This dependence is depicted in Fig. 5 and 6. In a typical experimental procedure the E^g/E^0

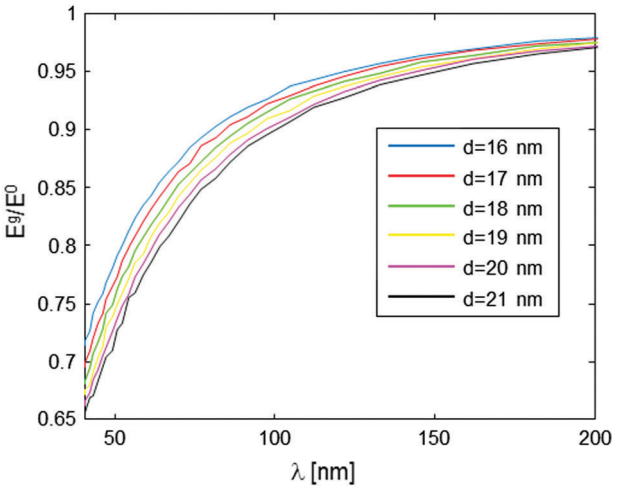

Fig. 4 Numerical simulation of E^g/E^0 evaluated at a 10 ms time evolution period as a function of gradient magnitude λ, for various values of spin pair distance, d. The simulation assumes a sample with a molecular concentration of 10^{14} molecules per cm^3 (0.16 μM), and $K_{ex} = 3.35 \times 10^5$ Hz nm^3.

data would be collected at a fixed Δ value of ~10 ms, for several values of $g(\lambda)$, and then the experimental curve of E^g/E^0 *vs.* λ would be fitted to the simulated data of Fig. 4. The calculation of such theoretical curves using current-day PCs can take several hours, meaning that the total fitting procedure can take around a day.

In order to properly extract d based on an experimentally-measured curve, it is therefore necessary to have a good knowledge of C and K_{ex}. The knowledge of C (for a homogenous sample) is trivial, and furthermore, if C is small enough its exact value is of negligible importance (see Fig. 5). On the other hand, the value of K_{ex} cannot be calculated accurately[22,24] and, as can be seen in Fig. 6, it may affect the nature of the measured plot. Our recent experiments with phosphorus-doped ^{28}Si:P

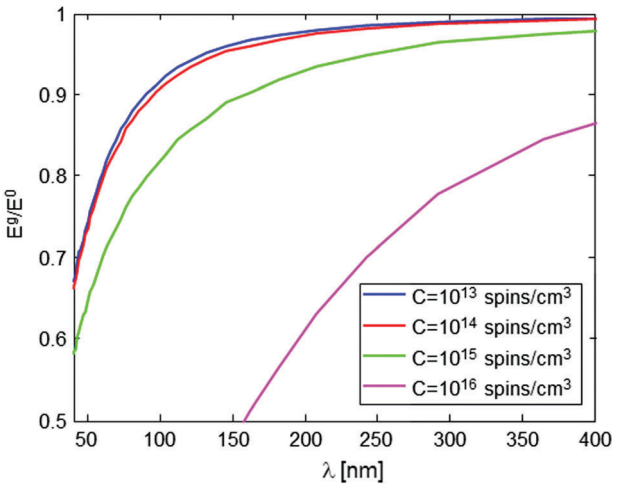

Fig. 5 Numerical simulation of E^g/E^0 evaluated at a 10 ms time evolution period as a function of gradient magnitude λ, for various values of sample concentration. The simulation assumes a sample with an intramolecular spin-pair distance of d = 20 nm, and $K_{ex} = 3.35 \times 10^5$ Hz nm^3.

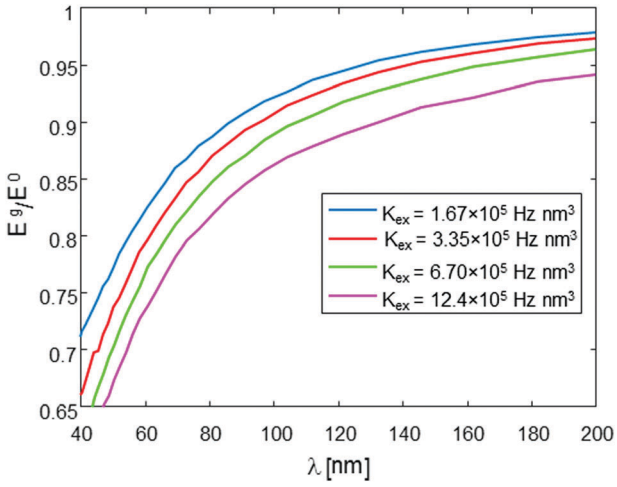

Fig. 6 Numerical simulation of E^g/E^0 evaluated at 10 ms time evolution period as a function of gradient magnitude λ, for various values of flip-flop exchange rate, K_{ex}. The simulation assumes a sample with an intramolecular spin-pair distance of d = 20 nm, and molecular concentration of 10^{14} molecules per cm^3.

have managed to measure K_{ex} for the first time, and this type of work can be also employed for the present challenge of evaluating d. For example, K_{ex} could be extracted from the decay curves of known samples with known d and C values, and then assumed not to change when switching to the sample with an unknown d, if the same solvent and the same temperature are used for the measurement. Alternatively, it is possible to use experimental E^g/E^0 *vs.* λ data on the molecules of interest with known concentration, but with single rather than two spin labels, and subsequently find K_{ex} which provides the best fit of the theoretical curve to the measured data. Clearly, however, much more work is required along this line to develop a better understanding of the nature of this parameter and its dependence on the sample and environmental conditions.

Overall, it can be summarized that the accuracy of the method for determining d relies on two main parameters: the signal-to-noise-ratio (SNR) of the measured E^g/E^0 plots *vs.* λ for a given sample, and the *a priori* knowledge of K_{ex}. Based on the results shown in Fig. 4, it is clear that an SNR of at least 100 is required to make possible a good differentiation between the plots for two different d values, varying by 1 nm one from the other. This, however, assumes that K_{ex} is well-known for the type of sample measured, or that its values are acquired using the procedure just described above. Any uncertainly in K_{ex} will be translated to uncertainly in the fitting of d. However, based on the results of Fig. 4 and 6 it is evident that even 100% uncertainly in K_{ex} would lead to only ~1–2 nm uncertainly in the fitted d value, so clearly this aspect is not very critical to the accuracy of the method.

One additional issue to consider is the possibility of having a distribution of several distances, and how this might affect the measured results. Fig. 7 addresses this question, simulating the same conditions as shown in Fig. 4, but assuming that d has Gaussian distribution around its mean value with standard deviation of 1, and 5 nm (Fig. 7a and b, respectively). It is

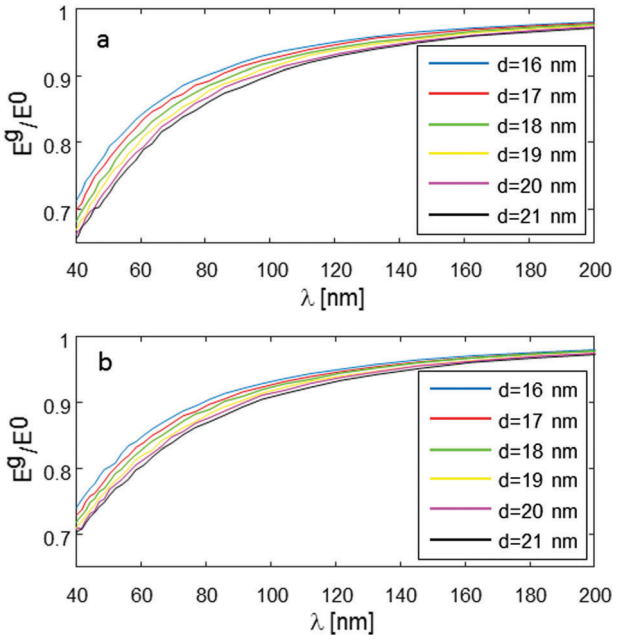

Fig. 7 Numerical simulation of E^9/E^0 with the same parameters as in Fig. 4, just assuming random distance Gaussian distribution around mean intramolecular spin-pair distance, d, with standard deviation of 1 nm (a) and 5 nm (b).

evident that for a small standard deviation (1 nm, Fig. 7a), there are very small differences compared to the original plots, for single d value (Fig. 4). However, for a relatively large standard deviation, of 5 nm (Fig. 7b), there are clear differences, with the larger average d values having smaller signal reduction than in the original plots of Fig. 4. The implication of this behavior is that it would probably be difficult to get accurate (better than ~10%) readings of the average d in such cases of molecules having very broad distance distribution of the intramolecular spin-pair distance.

4. Experimental feasibility

In this section we examine the feasibility of actually measuring spin diffusion and extracting the intramolecular spin-pair distance from it using the above-described experimental approach. There are two significant experimental difficulties that should be considered. The first experimental difficulty is applying the powerful and short magnetic field gradient pulses and subsequently collecting the ESR signal with minimal interferences. As noted above, typical values of the required gradients' magnitude can range from 100–1000 T m^{-1}, while their duration should be not more than 1–2 μs, in order to be comparable to typical T_m of common spin labels at cryogenic temperatures. Such capabilities have been demonstrated in the past in our laboratory[35–37] and, as noted above, also in conjunction with our recent efforts where we succeeded in actually measuring spin diffusion in a solid sample of phosphorus-doped ^{28}Si.[20] It should be noted, however, that in order to apply such strong gradients over a short period of time, very compact resonators must be used that allow the involvement of miniature gradient coils with low inductance and high efficiency. Thus, for example, in our recent work with phosphorus-doped ^{28}Si, we employed a miniature dielectric disc resonator at Q-band with inner diameter of ~0.6 mm, outer diameter of ~1.1 mm, and height of ~0.2 mm. This implies that the available sample volume is limited to less than ~0.05 μl, which in turn limits the concentration sensitivity of the measurement, giving rise to the second significant experimental difficulty. As can be learned from our discussion above, to properly measure distances in the range of d ~ 20 nm, the sample concentration cannot exceed ~10^{15} spins per cm^3 (≈1.6 μM). A quantitative estimation of the available concentration sensitivity for trityl-type samples measured at temperature of ~20–30 K (with T_1 ~ 10 ms) using such Q-band dielectric disc resonator as described above, can be made applying the known expression for spin sensitivity.[38,39] Such calculation predicts concentration sensitivity values of ~1 μM, with a signal-to-noise-ratio of 10 by acquiring signal over a few seconds of averaging time. Thus, the same probe employed for our recent diffusion measurements can in principle be used for the new distance measurement procedure we suggest here. One additional point of relevance with regards to spin sensitivity is that the level of dipolar signal oscillation measured in common DEER experiments can be smaller than the actual full ESR echo signal of the sample by factors ranging from 2 to even 100. Here, however, the spin diffusion measurements take the advantage of looking at the full stimulated echo signal (which is just a factor of 2 smaller than the Hahn echo signal), thereby significantly contributing to the sensitivity of the technique.

5. Summary and outlook

A new approach was described for the measurement of the distance, d, between a pair of spin labels on a molecule. The feasibility of this approach for measuring d values of ~20 nm was presented and discussed based on a theoretical (numerical) simulation of spin diffusion, as well as by analyzing the required experimental capabilities and setup for implementing it. A successful realization of this new approach can extend the available measureable distance between intramolecular labels by a factor of at least ~2, which can have broad implications in the field of structural biology. A practical experimental demonstration of this approach would require the synthesis of a doubly-labeled macromolecule, with a well-defined intramolecular spin-pair distance, using spin labels that have a relatively narrow line to increase as much as possible the rate of the flip-flop. A good possible candidate for such future experiment is double-stranded DNA, which is very rigid (having a persistence length of ~50 nm[40]), labeled with a trityl radical.[13]

Appendix: numerical simulation of the echo magnitude decay due to spin diffusion

The numerical simulation follows many (typically ~100) bi-radical molecules, randomly located in the 3D sample space, as they

evolve throughout the pulse sequence of Fig. 1b. The calculation is repeated ~1000 times, each time with different random locations of the molecules, and the results are averaged. Our experiments[20] can measure the value of the stimulated echo intensity with gradients, E^g, normalized to the echo intensity without gradients, E^0, thereby virtually canceling out the effects of T_1 and T_m relaxation on the signal. The molecules are first randomly placed in the sample with a mean distance that corresponds to their bulk concentration. Each molecule comprises two spins that are separated by a distance d between them, with random relative orientation. Following this, the simulation applies a pulsed magnetic field gradient that creates a corresponding spatially-dependent phase profile for the spins in the sample along the z-axis (parallel to the applied static field, B_0). The spins are then given the opportunity to evolve during the evolution time with small time steps Δt (typically 1–10 μs). In terms of the simulation, this means that at each time step a given spin has a chance to flip-flop with other spins. The flip-flop process between spins j and k during a given short time step, is simulated as a random stochastic Markovian event with a probability of $\Delta t \times K_{ex}^2(3\cos^2\theta_{jk} - 1)^2/r_{jk}^6$, (based on eqn (2), with $K_{ex} \equiv \sqrt{\frac{\pi}{8} f_{jk}(0)}\left[\frac{\mu_0}{4\pi}\hbar\gamma_j\gamma_k\right]$). This stochastic approach was preferred over a deterministic oscillation between the two states (as can be expected for a purely environmentally-isolated two spin system[23]), since in our opinion it represents better the average nature of events occurring in such multi-spin interacting system. Similar simulation, using this stochastic approach, but without the interaction of closely-spaced spin pairs, showed good correspondence with the Stekel–Tanner predictions in our previous work.[20] Following the evolution time, the spins are then subjected to another gradient pulse that unwinds the phase profile generated by the first pulse. If no significant spin diffusion occurred *via* flip-flops, the complex sum magnitude of all the spins in the sample should amount to their number. However, if many flip-flop events occurred, the complex sum becomes lower than the maximal value, as measured by our PGSE sequence. To fit the future experimental results (of E^g/E^0), two possible adjustable parameters can be used in this numerical simulation: d and K_{ex}. As noted in the text, K_{ex} should be calibrated based on some reference samples to provide a good fit to d.

Acknowledgements

This work was partially supported by grant #310/13 from the Israel Science Foundation (ISF), grant #FA9550-13-1-0207 from the Air Force Office of Scientific Research (AFOSR), grant #3-12372 from the Israeli Ministry of Science, and by the Russell Berrie Center for Nanotechnology at the Technion.

Notes and references

1 G. Jeschke, *Annu. Rev. Phys. Chem.*, 2012, **63**(63), 419–446.
2 P. P. Borbat, H. S. Mchaourab and J. H. Freed, *J. Am. Chem. Soc.*, 2002, **124**, 5304–5314.
3 G. Jeschke, M. Pannier, A. Godt and H. W. Spiess, *Chem. Phys. Lett.*, 2000, **331**, 243–252.
4 O. Duss, E. Michel, M. Yulikov, M. Schubert, G. Jeschke and F. H. T. Allain, *Nature*, 2014, **509**, 588–592.
5 O. Duss, M. Yulikov, G. Jeschke and F. H. T. Allain, *Nat. Commun.*, 2014, **5**, 3669.
6 N. S. Alexander, A. M. Preininger, A. I. Kaya, R. A. Stein, H. E. Hamm and J. Meiler, *Nat. Struct. Mol. Biol.*, 2014, **21**, 56–63.
7 E. R. Georgieva, P. P. Borbat, C. Ginter, J. H. Freed and O. Boudker, *Nat. Struct. Mol. Biol.*, 2013, **20**, 215–221.
8 I. D. Sahu, R. M. McCarrick, K. R. Troxel, R. F. Zhang, H. J. Smith, M. M. Dunagan, M. S. Swartz, P. V. Rajan, B. M. Kroncke, C. R. Sanders and G. A. Lorigan, *Biochemistry*, 2013, **52**, 6627–6632.
9 M. T. Lerch, Z. Y. Yang, E. K. Brooks and W. L. Hubbell, *Proc. Natl. Acad. Sci. U. S. A.*, 2014, **111**, E1201–E1210.
10 M. Azarkh, V. Singh, O. Oklre, I. T. Seemann, D. R. Dietrich, J. S. Hartig and M. Drescher, *Nat. Protoc.*, 2013, **8**, 131–147.
11 P. P. Borbat, E. R. Georgieva and J. H. Freed, *J. Phys. Chem. Lett.*, 2013, **4**, 170–175.
12 G. W. Reginsson, N. C. Kunjir, S. T. Sigurdsson and O. Schiemann, *Chem. – Eur. J.*, 2012, **18**, 13580–13584.
13 G. Y. Shevelev, O. A. Krumkacheva, A. A. Lomzov, A. A. Kuzhelev, O. Y. Rogozhnikova, D. V. Trukhin, T. I. Troitskaya, V. M. Tormyshev, M. V. Fedin, D. V. Pyshnyi and E. G. Bagryanskaya, *J. Am. Chem. Soc.*, 2014, **136**, 9874–9877.
14 W. Richard, A. Bowman, E. Sozudogru, H. El-Mkami, T. Owen-Hughes and D. G. Norman, *J. Magn. Reson.*, 2010, **207**, 164–167.
15 P. A. S. Cruickshank, D. R. Bolton, D. A. Robertson, R. I. Hunter, R. J. Wylde and G. M. Smith, *Rev. Sci. Instrum.*, 2009, **80**, 103102.
16 G. Jeschke, in *Structural Information from Spin-Labels and Intrinsic Paramagnetic Centres in the Biosciences*, ed. C. R. Timmel and J. R. Harmer, Springer Berlin Heidelberg, Berlin, Heidelberg, 2013, pp. 83–120, DOI: 10.1007/430_2011_61.
17 G. Jeschke, A. Koch, U. Jonas and A. Godt, *J. Magn. Reson.*, 2002, **155**, 72–82.
18 Y. W. Chiang, P. P. Borbat and J. H. Freed, *J. Magn. Reson.*, 2005, **172**, 279–295.
19 H. Sato, S. E. Bottle, J. P. Blinco, A. S. Micallef, G. R. Eaton and S. S. Eaton, *J. Magn. Reson.*, 2008, **191**, 66–77.
20 E. Dikarov, O. Zgadzai, Y. Artzi and A. Blank, *Phys. Rev. Appl.*, 2016, **6**, 044001.
21 N. Bloembergen, *Physica*, 1949, **15**, 386–426.
22 M. Ernst and B. Meier, *Stud. Phys. Theor. Chem.*, Elsevier, 1998, vol. 84, pp. 83–121.
23 A. Abragam, *The principles of nuclear magnetism*, Clarendon Press, Oxford, 1961.
24 J. Dolinsek, P. M. Cereghetti and R. Kind, *J. Magn. Reson.*, 2000, **146**, 335–344.
25 J. E. Tanner, *J. Chem. Phys.*, 1970, **52**, 2523–2526.
26 H. Y. Carr and E. M. Purcell, *Phys. Rev.*, 1954, **94**, 630–638.
27 E. O. Stejskal and J. E. Tanner, *J. Chem. Phys.*, 1965, **42**, 288–292.

28 P. T. Callaghan, A. Coy, D. Macgowan, K. J. Packer and F. O. Zelaya, *Nature*, 1991, **351**, 467–469.
29 P. T. Callaghan, *Translational dynamics and magnetic resonance: principles of pulsed gradient spin echo NMR*, Oxford University Press, Oxford, New York, 2011.
30 H. A. Reich, *Phys. Rev.*, 1963, **129**, 630–643.
31 J. R. Thompson, E. R. Hunt and H. Meyer, *Phys. Lett. A*, 1967, **A25**, 313–314.
32 W. R. Zhang and D. G. Cory, *Phys. Rev. Lett.*, 1998, **80**, 1324–1327.
33 K. W. Eberhardt, S. Mouaziz, G. Boero, J. Brugger and B. H. Meier, *Phys. Rev. Lett.*, 2007, **99**, 227603.
34 G. G. Maresch, A. Grupp, M. Mehring, J. U. Vonschutz and H. C. Wolf, *J. Phys.*, 1985, **46**, 461–464.
35 Y. Talmon, L. Shtirberg, W. Harneit, O. Y. Rogozhnikova, V. Tormyshev and A. Blank, *Phys. Chem. Chem. Phys.*, 2010, **12**, 5998–6007.
36 A. Blank, Y. Talmon, M. Shklyar, L. Shtirberg and W. Harneit, *Chem. Phys. Lett.*, 2008, **465**, 147–152.
37 L. Shtirberg and A. Blank, *Concepts Magn. Reson., Part B*, 2011, **39**, 119–127.
38 Y. Twig, E. Dikarov and A. Blank, *Mol. Phys.*, 2013, **111**, 2674–2682.
39 L. Shtirberg, Y. Twig, E. Dikarov, R. Halevy, M. Levit and A. Blank, *Rev. Sci. Instrum.*, 2011, **82**, 043708.
40 A. Brunet, C. Tardin, L. Salome, P. Rousseau, N. Destainville and M. Manghi, *Macromolecules*, 2015, **48**, 3641–3652.